

Cleveland State University

EngagedScholarship@CSU

Scholarship Collection

Books

5-1995

Vibration Analysis of a Split Path Gearbox

Timothy L. Krantz

Lewis Research Center, Cleveland OH

Majid Rashidi

Cleveland State University, M.RASHIDI@csuohio.edu

Follow this and additional works at: <https://engagedscholarship.csuohio.edu/scholbks>



Part of the [Aerodynamics and Fluid Mechanics Commons](#)

How does access to this work benefit you? Let us know!

Recommended Citation

Krantz, Timothy L. and Rashidi, Majid, "Vibration Analysis of a Split Path Gearbox" (1995). *Scholarship Collection*. 129.

<https://engagedscholarship.csuohio.edu/scholbks/129>

This Book is brought to you for free and open access by the Books at EngagedScholarship@CSU. It has been accepted for inclusion in Scholarship Collection by an authorized administrator of EngagedScholarship@CSU. For more information, please contact library.es@csuohio.edu.



NASA
Technical Memorandum 106875
AIAA-95-3048

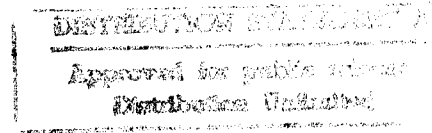
Army Research Laboratory
Technical Report ARL-TR-723

Vibration Analysis of a Split Path Gearbox

Timothy L. Krantz
Vehicle Propulsion Directorate
U.S. Army Research Laboratory
Lewis Research Center
Cleveland, Ohio

and

Majid Rashidi
Cleveland State University
Cleveland, Ohio



Prepared for the
31st Joint Propulsion Conference
cosponsored by AIAA, SAE, and ASME
San Diego, California, July 10-12, 1995

19960202 020



National Aeronautics and
Space Administration

DTIC QUALITY INSPECTED 1



VIBRATION ANALYSIS OF A SPLIT PATH GEARBOX

Timothy L. Krantz
U.S. Army Research Laboratory
Lewis Research Center
Cleveland, Ohio 44135

and

Majid Rashidi
Cleveland State University
Cleveland, Ohio 44115

Abstract

Split path gearboxes can be attractive alternatives to the common planetary designs for rotorcraft, but because they have seen little use, they are relatively high risk designs. To help reduce the risk of fielding a rotorcraft with a split path gearbox, the vibration and dynamic characteristics of such a gearbox were studied. A mathematical model was developed by using the Lagrangian method, and it was applied to study the effect of three design variables on the natural frequencies and vibration energy of the gearbox. The first design variable, shaft angle, had little influence on the natural frequencies. The second variable, mesh phasing, had a strong effect on the levels of vibration energy, with phase angles of 0° and 180° producing low vibration levels. The third design variable, the stiffness of the shafts connecting the spur gears to the helical pinions, strongly influenced the natural frequencies of some of the vibration modes, including two of the dominant modes. We found that, to achieve the lowest level of vibration energy, the natural frequencies of these two dominant modes should be less than those of the main excitation sources.

Introduction

The performance of a rotorcraft drive system has a significant impact on the vehicle's payload and range, passenger comfort and safety, operating cost, and readiness. To improve the drive system, designers strive for systems that are lighter in weight, quieter, and more reliable than the current state-of-the-art designs. An important decision that must be made early in the design of the drive system is the selection of the gearing arrangement. The most common choice for the final gear stage of a helicopter main rotor transmission has been a planetary stage, which features an output shaft driven by several planets. With this planetary arrangement, power is transmitted through multiple load paths. The multiple load paths reduce the weight of the gear train since the size of a gear is determined by the gear tooth loads rather than the total torque. Planetary stage designs

for rotorcraft have been studied and developed extensively through decades of experience.

An alternative to a planetary stage is a split path stage. To date, split path stages (sometimes called split torque) have seldom been used in rotorcraft. Although a split path design features only two load paths rather than the three to six typical of planetary designs, it can provide a larger speed reduction at the final stage and thus the weight of the drive train can be reduced. White¹⁻³ advocated using split torque gear trains for rotorcraft because they can offer such advantages as lower weight, fewer parts, higher reliability, reduced noise, and reduced power losses. However, a lack of experience has inhibited their use in helicopters since these designs have been considered costlier to develop and riskier to use than the planetary designs.

Recently, several researchers have studied and developed split path transmission technology. Heath and Bossler⁴ reported on the study and development of a design that features the use of face gears. Hochmann et al.⁵ studied the tooth loading distribution of spur and double helical gear pairs of a split path design. Krantz and Rashidi^{6,7} studied the dynamics of a design that featured a beam mechanism which automatically balanced the power between the two load paths. Kish⁸ reported on the study and development of a split path design for a helicopter; that work included extensive laboratory testing, and a similar design was selected for use in the U.S. Army RAH-66 Comanche helicopter. Kahraman⁹ concluded, after using a dynamic analysis to study multi-mesh gear trains, that the positions of the gears had a significant influence on dynamic response of such systems.

In this investigation, the vibration and dynamic characteristics of a split path gearbox were studied. A mathematical model of the gear train was derived to study the effect of design variables on the natural frequencies and levels of vibration energy of the gearbox. The results of studying three variables, shaft angle, mesh phasing, and compound shaft stiffness, are presented.

Description of the Gearbox

The gearbox studied here was developed and tested as part of the Advanced Rotorcraft Transmission (ART) Program.⁸ It is representative of technology for a complete main rotor transmission for an advanced cargo aircraft with three engines. The gearbox was built at half scale and includes only the final two stages for one engine. (The first stage of the complete transmission is a 3.04:1 ratio spiral bevel mesh.) A cross section of the gearbox is shown in Fig. 1, and the gearing arrangement is shown schematically in Fig. 2. The gearbox features a high-contact-ratio involute spur pinion with 26 teeth driving 2 gears of 101 teeth. The input power is split between the two spur gears. The spur gears share common shafts with double helical pinions of 13 teeth. The combination of a spur gear and double helical pinion on a common shaft is designated a "compound shaft." The double helical pinions drive the output gear, called the bull gear, which has 127 teeth. The overall speed reduction of the test gearbox is 37.9:1.

Split path designs used in or proposed for helicopters have a device that ensures proper sharing of the load.⁸ Consider the gear train of Fig. 2. If it consisted of infinitely rigid parts, then to transmit power through both power paths, the gears of the

compound shafts would have to be clocked or indexed such that all the gear meshes would be in contact under a nominal light load. Any small error in the geometry of these rigid parts would result in all of the power being transmitted through one power path. In reality, parts have some flexibility, and at a given design torque, there is an optimal indexing of the gears that produces equal sharing of the loads. Many methods have been proposed as a way to minimize the effect of manufacturing errors on load sharing in split path transmissions. One such device investigated in the ART program was a torsionally compliant compound shaft. The shaft had a special geometry and was made of elastomer-steel laminates that provided high torsional compliance with high lateral stiffness. A torsionally stiff compound shaft was also tested for comparison. From this study, Kish⁸ concluded that (1) excellent load sharing can be achieved by using a torsionally compliant compound shaft and (2) acceptable (but less than excellent) load sharing can be achieved without a load sharing device so long as manufacturing and installation tolerances are adequately controlled. Although the compliant shaft provided excellent load sharing, it did not meet operational requirements. The elastomer-steel laminates were adversely affected by temperature cycles, and thus, the function of the device was degraded. Since some other

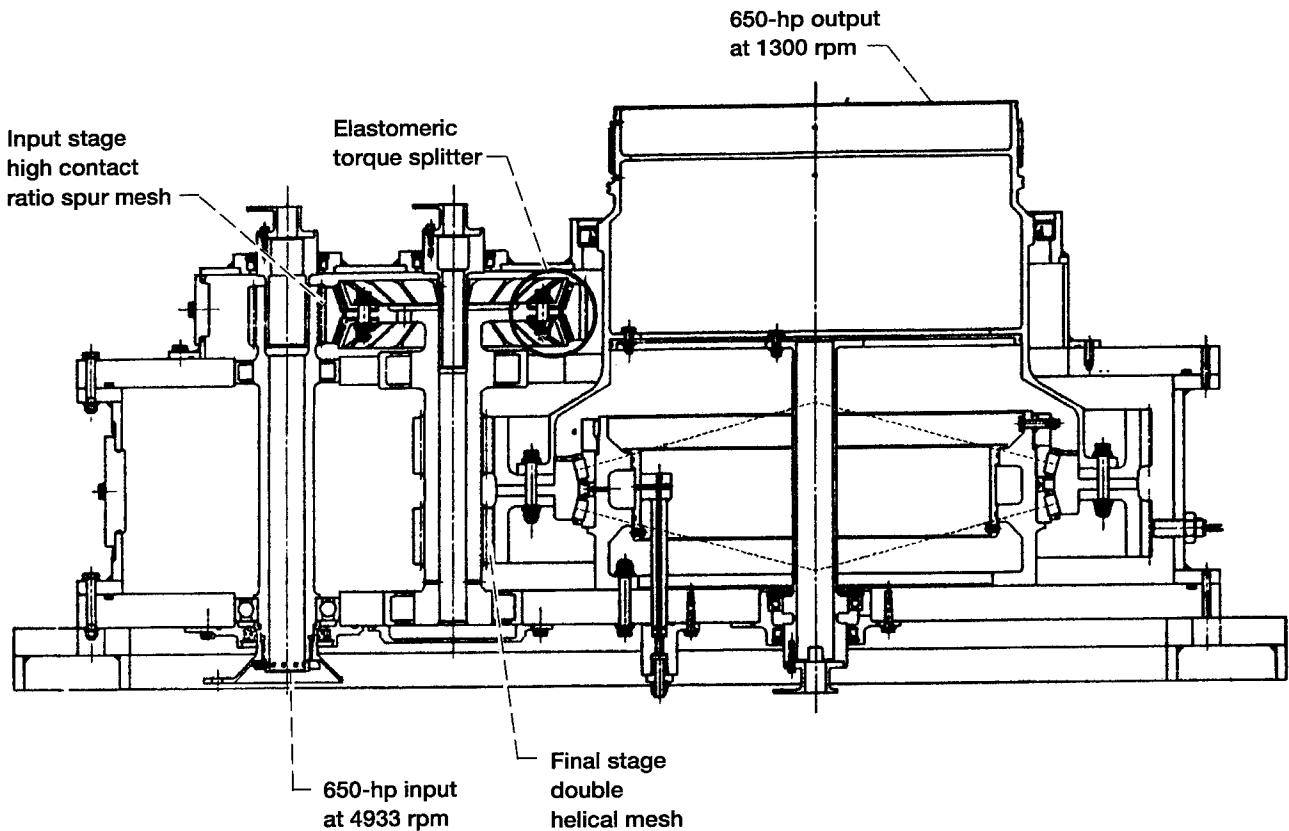
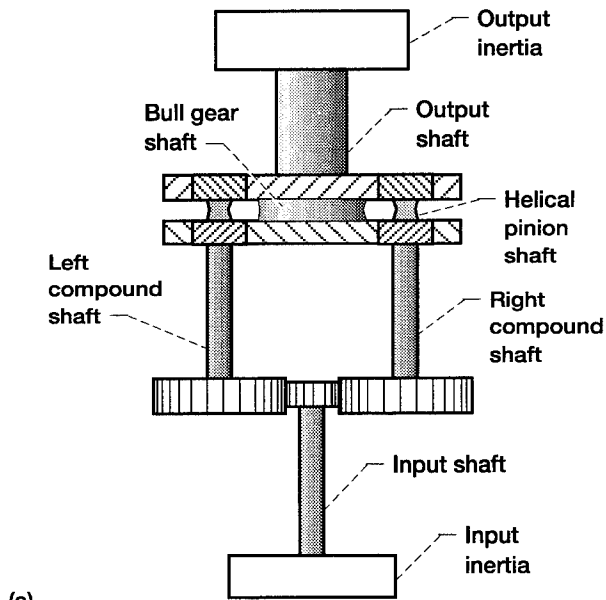
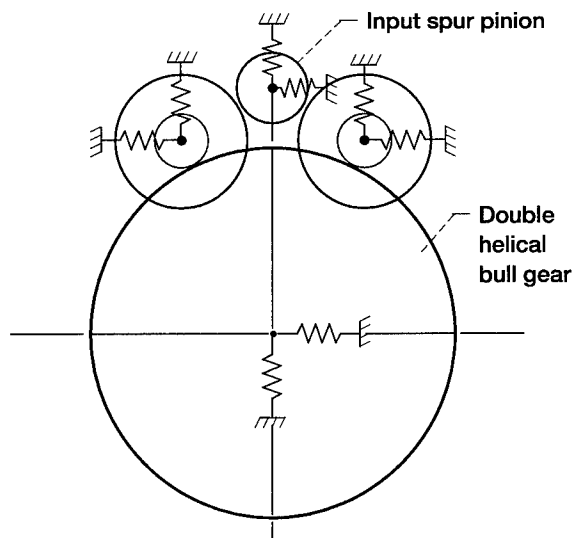


Fig. 1.—Cross-sectional view of the ART split path test gearbox^[8].



(a)

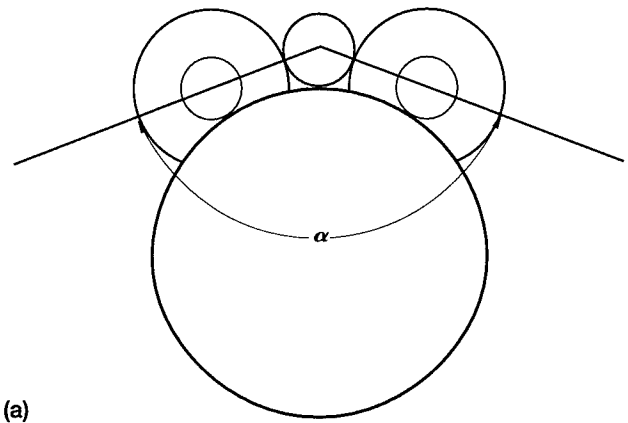


(b)

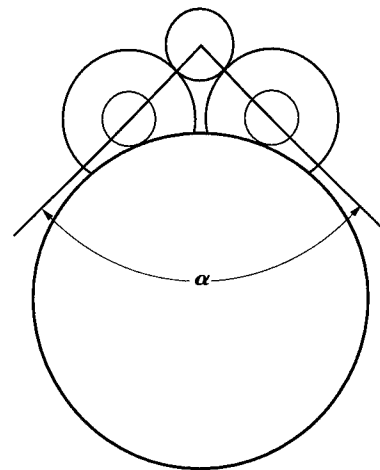
Fig. 2.—Schematic representation of the ART split path test gearbox. (a) Top view showing shafts and inertias. (b) Front view showing lateral supports.

version of a torsionally compliant shaft might be considered for future designs, the compound shaft stiffness was considered as a design variable in this study.

In addition to shaft compliance, we chose two properties of the gearbox as design variables and studied their impact on dynamic response: the first was the shaft angle (Fig. 3), which defines the locations of the gear centers; the second was mesh phasing (Fig. 4), which defines the relative timing of the varying, periodic mesh properties. In practice, for a given set of gears and center distances, the mesh phasing is defined by the shaft angle. Here, however, they were considered as independent variables for the purpose of analysis.



(a)



(b)

Fig. 3.—Two assemblies of same gears at different input shaft angles. (a) Shaft angle of 140°. (b) Shaft angle of 90°.

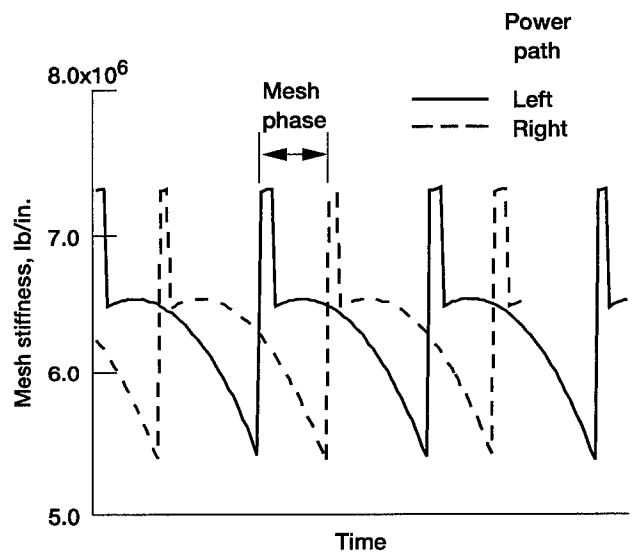


Fig. 4.—Time-varying spur mesh stiffness showing mesh phase.

Mathematical Modeling

The model outlined here is similar to one we previously developed for another transmission. Further details of the modeling method can be found in Refs. 6 and 7.

A lumped mass and spring system was chosen to model the transmission. An inertia element was included for each gear, with each half of the double helical gears considered to be a separate inertia. Input and output inertias were included in the model. Torsional spring elements were also included, one each for the input shaft, output shaft, for each of the two compound shafts, and each of the shafts joining the halves of the double helical gears. Each gearshaft was supported by a pair of lateral springs. This implies the simplifying assumption that the gearshafts may move laterally but do not tilt. Axial motions were not considered in this study. A single lumped mass was included for each gearshaft. Each gear mesh was modeled by a stiffness and displacement element pair (Fig. 5) attached to rigid base circles, thereby automatically accounting for the operating pressure angles. All stiffness elements were considered linear and, in the case of the mesh elements, time-varying. The displacement elements of the gear mesh were included in the model to simulate pitch errors, runout, and other components of static transmission error not attributable to stiffness effects.

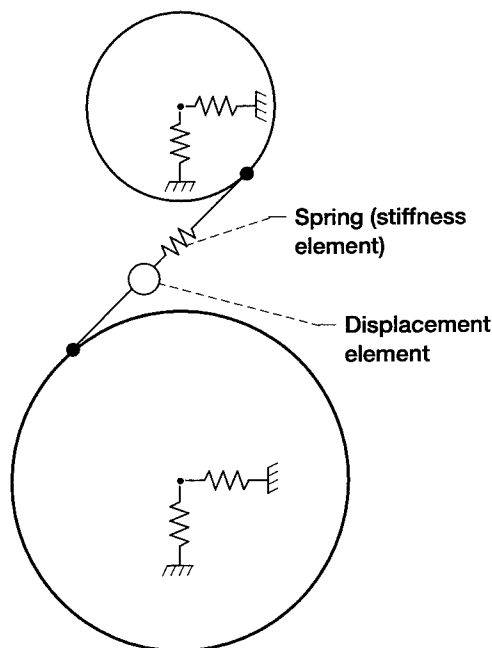


Fig. 5.—Gear dynamics model.

In this work, damping was not included. Although structural damping is thought to be significant in gear systems and is often modeled by adding equivalent viscous dampers to the model, the analogy between structural and viscous damping is strictly valid only for pure harmonic excitation.¹⁰ Here, we chose to use a model with no damping since the goal was to predict relative changes in the levels of vibration as the design variables were changed, not to predict absolute levels of vibration.

A set of equations of motion for the model were derived by the standard Lagrangian method:

$$\frac{d}{dt} \left(\frac{\partial L}{\partial \dot{q}_j} \right) - \frac{\partial L}{\partial q_j} = Q_j \quad (j = 1, 2, \dots, 19)$$

where $L = T - V$; T = total kinetic energy; V = total potential energy; q_j = generalized coordinate; and Q_j = generalized forcing function. Functions defining the displacement elements of the mesh model were included on the right side of the Lagrangian equation as part of the generalized forcing function Q_j .

The time-varying mesh stiffnesses were determined by applying the techniques of Cornell.¹¹ First we determined the stiffness of a pair of spur gear teeth as a function of contact position. Then we considered the kinematics to determine the number of teeth in contact and the contact positions. Finally, we summed the stiffnesses of all contacting teeth to yield the mesh stiffness as a function of gear position. The helical gears were modeled as a series of staggered spur gears so that Cornell's method for spur gears could be applied. The time-varying stiffness function for the spur mesh stiffness elements is shown in Fig. 4. The positions of sudden change in the stiffness function are positions of change in the number of teeth in contact. These sudden changes in stiffness are a major source of vibration in geared systems.

The time-varying mesh displacement elements were defined as the sum of two sinusoidal functions whose frequencies are equal to the rotation frequencies of the two meshing gears. The elements were defined this way to simulate the effects of typical runout and accumulated pitch errors on the motions of the system.

After applying the Lagrangian technique, we made the resulting set of equations nondimensional to prepare them for a numeric solution. The mathematical model derived was a set of 19 equations with linear but time-varying coefficients. The system of equations is semidefinite, having a rigid body mode

in torsion. The sources of forced vibration for the system used in this study were the time-varying mesh stiffness and displacement elements. These elements were defined such that the static transmission errors of the analytical model were similar to those of typical gearboxes. No external varying forcing functions or mass imbalance effects were considered in this study.

Analysis Techniques

Both time domain and frequency domain calculations were done to study the system of equations of the mathematical model. We calculated the system's natural frequencies to study behavior in the frequency domain, and we integrated the equations numerically using a fifth/sixth order Runge-Kutta method¹² to study behavior in the time domain. To integrate, one needs an appropriate set of initial conditions. In this investigation, we set all generalized coordinates equal to zero, and zero forces and torques were applied to the system. Thus, zero potential energy was stored in the spring elements at time equal to zero. This initial condition corresponds to the gearbox operating at speed with negligible load and with negligible vibration. The transition from this known initial state to the full power condition was accomplished by gradually applying input and output torques to the system with a 0.05-sec ramp-up function. At any instant, torques corresponding to equal but opposite power were applied to the input and output inertias. The time step of the numeric integration was selected to be about 1/40th of the spur gear mesh period.

The procedure just described for the time domain studies yielded the system response to both the time-varying mesh properties and the ramp-up input and output torque functions. Since we were interested in obtaining the system response to the time-varying mesh only, a second set of time domain calculations were done with the mesh properties defined as constants equal to the time-averaged mean value. This gave the system response to just the ramp-up functions. Then, applying the principle of superposition, we subtracted the response to just the ramp-up functions from that of both excitations to determine the system response to the time-varying mesh properties only. From the system response for typical gearbox excitations, figures of merit, based on the vibration energy of the system, were calculated as follows to compare design options:

$$E_i = \frac{\int_{t_1}^{t_2} \frac{1}{2} k_i \beta^2 dt}{(t_2 - t_1)} \quad (i = 1, 2, \dots, 21)$$

Here, E_i is the vibration energy figure of merit for spring i ; k_i is the spring constant; and β is the change in length of the

spring element from its mean length during the time from t_1 to t_2 . For torsional motions, the equation was applied directly. For lateral motions, the two springs supporting each shaft were converted to a single radial stiffness value, and the lateral motions were converted from Cartesian to polar coordinates before the figure of merit was calculated. The figure of merit is a measure of the vibration energy passing through a shaft or shaft support.

Parametric Studies and Results

The ART split path test gearbox with a torsionally compliant compound shaft⁸ (Fig. 1) was the baseline design for this study. Variations of this design were also studied by changing one design variable at a time to explore the impact of the variable on vibration modes and vibration energy levels of the gearbox.

Frequency Domain Studies

The input pinion shaft angle α (Fig. 3) was considered as a design variable. For a given set of gears and center distances, it defines the locations of the gear centers. The natural frequencies of the gearbox were calculated as the shaft angle was varied from 80° to 180° (see Fig. 6). Note that many of the natural frequencies remain essentially constant as the shaft angle is varied. Also, it is significant that many modes are within the range of the gearbox meshing fundamental frequencies and primary harmonics, the spur fundamental frequency being 2140 Hz and the helical being 275 Hz. In practice, the selection of shaft angle would be dictated not only by predicted dynamic

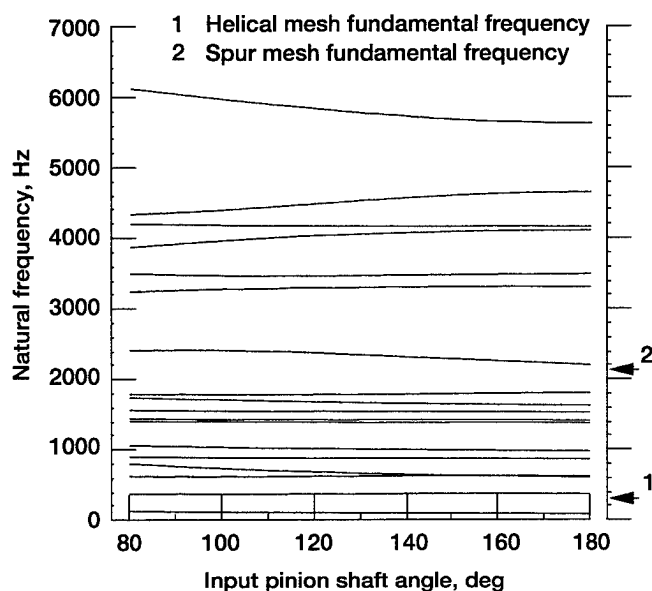


Fig. 6.—Effect of shaft angle on natural frequencies and relationships to mesh frequencies.

response but also by other requirements such as gearbox envelope constraints, location of accessory drives, and static bearing loads, among others. With this in mind, and since many of the natural frequencies were not significantly changed by varying the shaft angle, we did no further studies on the effect of shaft angle. Also, we judged that for studying the effects of shaft stiffness and mesh phasing, the trends obtained with the baseline shaft angle would be similar to trends obtained with any practical shaft angle.

The compound shaft torsional stiffness was also considered as a design variable, and the natural frequencies of the gearbox were calculated as the shaft stiffness was varied from 1×10^6 to 8.8×10^6 in.-lb/rad (see Fig. 7). Although many of the natural frequencies did not change, the frequencies of some modes, especially modes 15 and 16, were significantly affected. As the shaft stiffness was increased, modes 15 and 16 approached the second harmonic of the spur mesh frequency of 4280 Hz. The effect of shaft stiffness was investigated further by using time domain studies; those results follow later in this report.

Time Domain Studies of the Effect of Mesh Phasing

The time domain response and vibration energy figures of merit E_i for the gearbox (defined earlier in this report) were calculated while the mesh phase was varied as a design variable over the full range of 0° to 360° . The results showed that mesh phasing has a very significant impact on the levels of vibration of the gearbox. Figure 8 shows the radial displacement of the gearshafts from their mean position versus time, for a mesh phase equal to 0° ; Fig. 9 shows the same for a mesh phase equal to 90° . The radial vibration of all the shafts increases significantly for the 90° phasing. Figures 10 and 11 show the dynamic

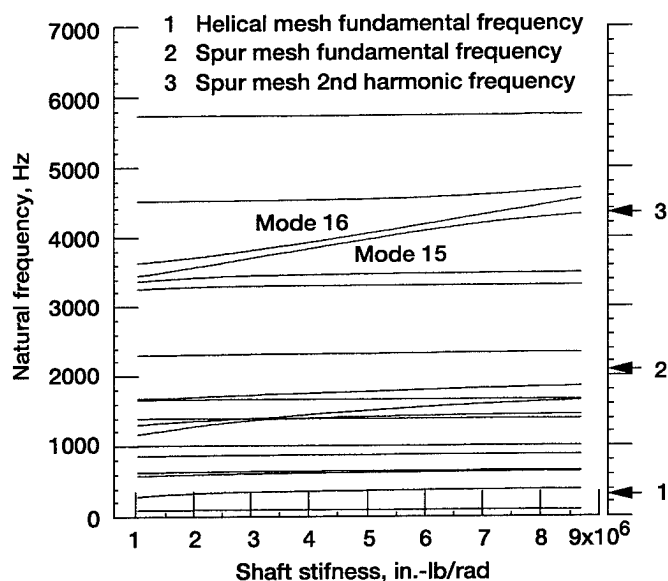


Fig. 7.—Effect of shaft stiffness on natural frequencies and relationships to mesh frequencies.

shaft torques for the compound shaft at 0° and 90° mesh phases, respectively. Although the torsional vibration in both shafts increases for 90° mesh phasing, the increase is more pronounced in the right compound shaft, or in other words, more pronounced in one of the two dual power paths.

A plot of the vibration energy figures of merit for the lateral vibrations (Fig. 12) shows that similar, relatively low vibration energy levels are produced for all shafts by 0° and 180° phasing. On the other hand, the 90° and the 270° mesh phasing produce levels of vibration nearly an order of magnitude greater. Note that the energy of the lateral vibrations of the dual power paths (right and left compound shafts) are essentially equal for all cases.

The vibration energy figures of merit for the torsional vibration (Fig. 13) exhibit more complex behavior than the lateral vibration figures of merit. As with the lateral vibration, 180° mesh phasing produces the lowest levels of vibration energy. It is very interesting to note that the matched sinusoidal shapes of the torsional and lateral vibration plots for the right compound shaft indicate the response is coupled. Conversely, the shapes of the left compound shaft torsional and lateral vibration plots are not matched.

Several differences were observed in the dynamic response of the left and right power paths. Whereas the geometry of the gearbox can be obtained by mirroring one-half of the gearbox about the center plane, the direction of one compound shaft does not mirror the other. Therefore, the loading of the two power paths are not symmetric, and force-coupled dynamic responses of the power paths can be expected to differ. A dynamic model, such as presented here, can assist in anticipating such differences.

Time Domain Studies of the Effect of Shaft Stiffness

The time domain response and vibration energy figures of merit E_i , as defined earlier in this report, were calculated for the gearbox while the two compound shaft stiffnesses were varied together over the range of 1×10^6 to 15×10^6 in.-lb/rad. A mesh phasing of 90° was used for all cases of this study. The results showed that shaft stiffness has a very significant impact on the levels of vibration of the gearbox. Figure 14 shows the variation in torsional vibration energy levels for five of the shafts of the gearbox as the compound shaft stiffness was varied. At a stiffness of about 6.8×10^6 in.-lb/rad, the natural frequency of the 16th mode of vibration coincides with the second harmonic of the spur mesh fundamental frequency. This results in the sharp increase in the torsional vibration of one of the two dual power paths (the left path). As the shaft stiffness is further increased toward 9.0×10^6 in.-lb/rad, the 15th mode of vibration is excited by the spur mesh second harmonic. This mode of vibration is very strong, causing large angular displacements in the right side power path.

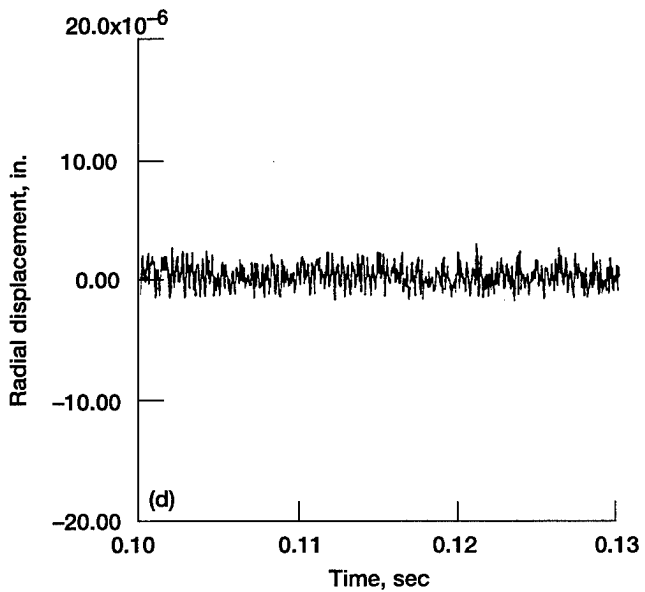
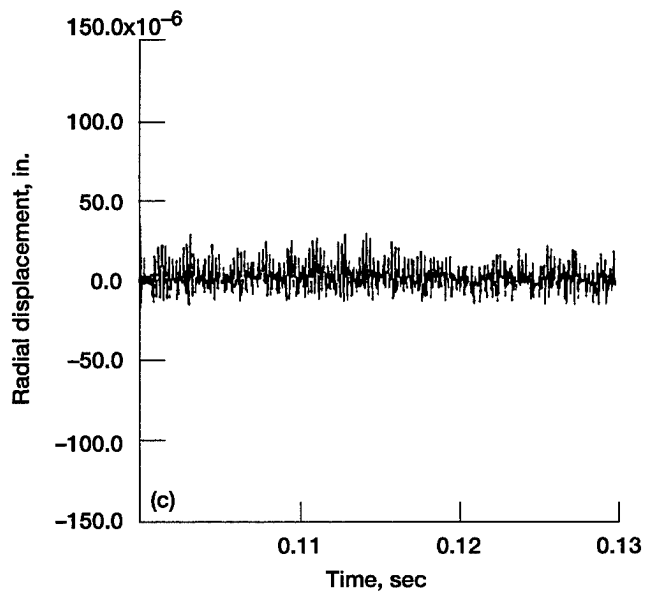
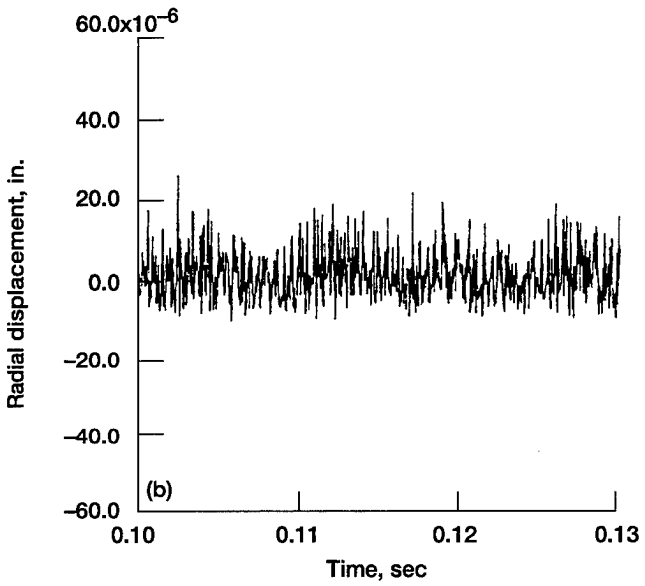
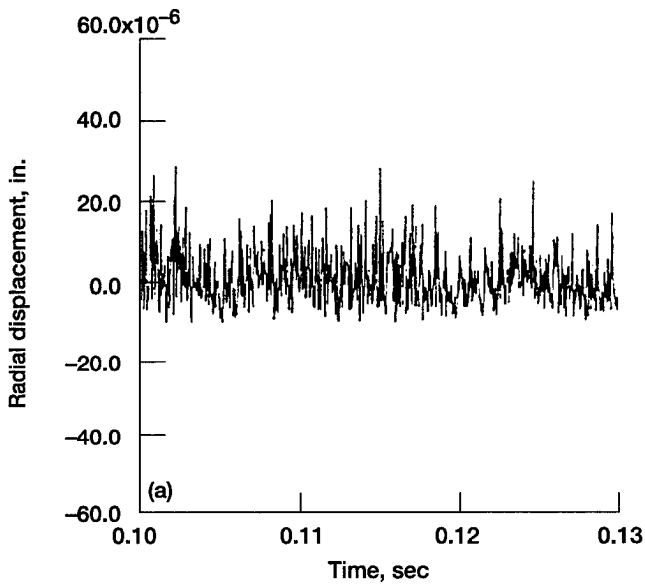


Fig. 8.—Gearshaft radial displacement from mean position for the case of 0° phasing of dual power paths showing vibration levels for all gearshaft supports. (a) Left compound shaft. (b) Right compound shaft. (c) Input pinion shaft. (d) Bull gear shaft.

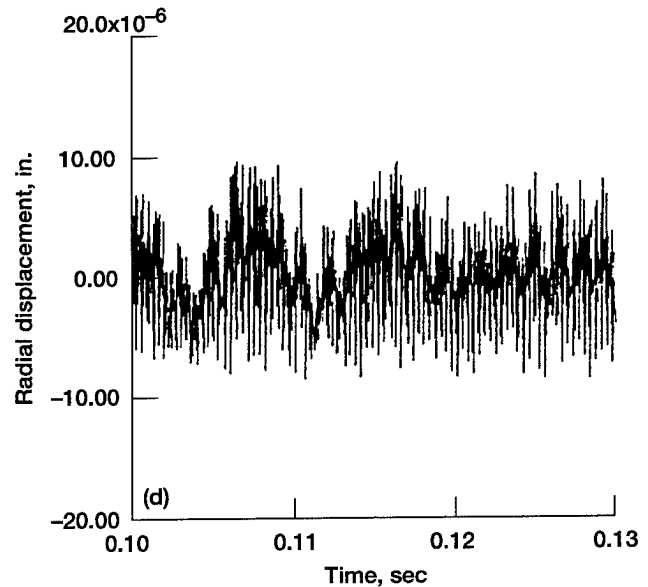
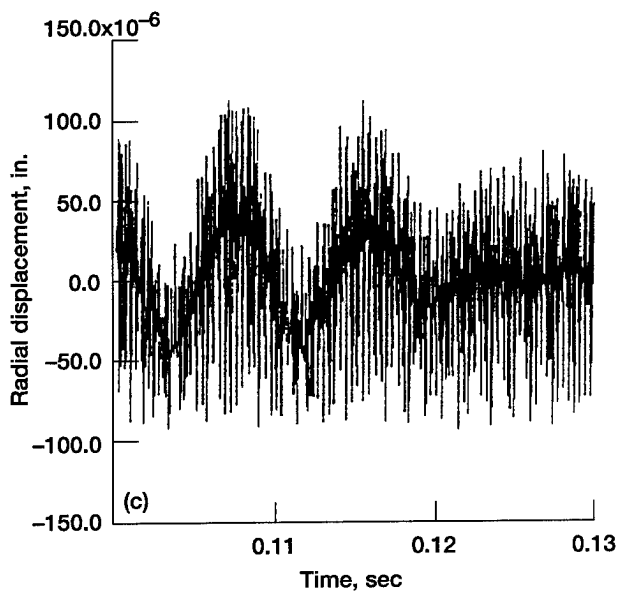
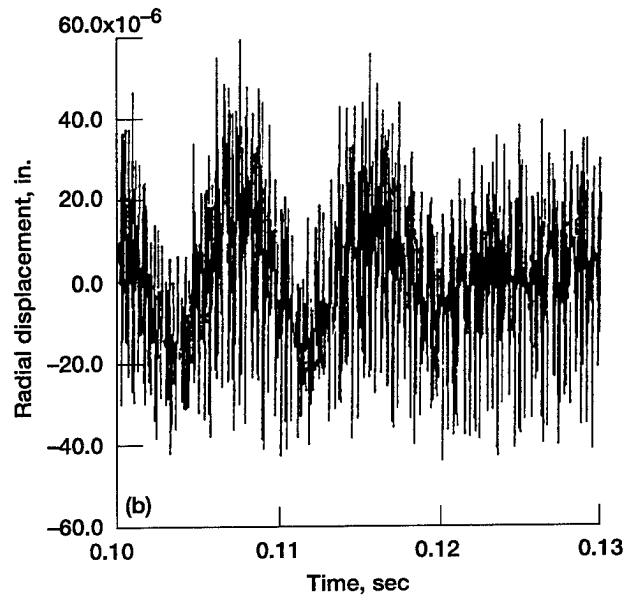
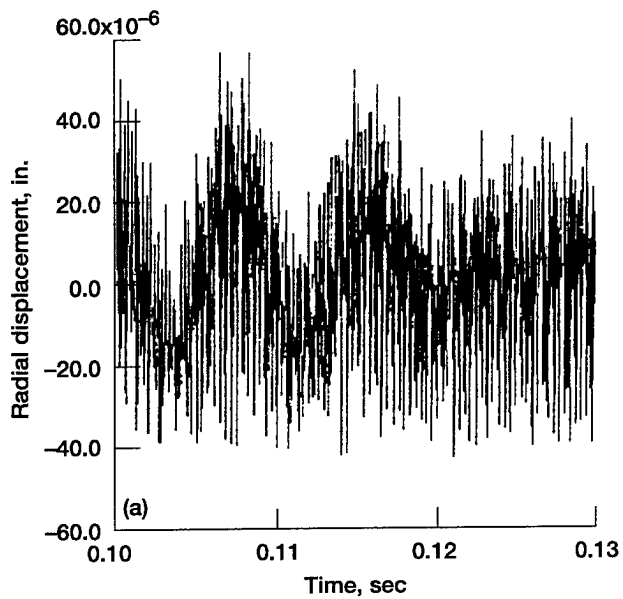


Fig. 9.—Gearshaft radial displacement from mean position for the case of 90° phasing of dual power paths showing large increase in vibration levels for all gearshaft supports. (a) Left compound shaft. (b) Right compound shaft. (c) Input pinion shaft. (d) Bull gear shaft.

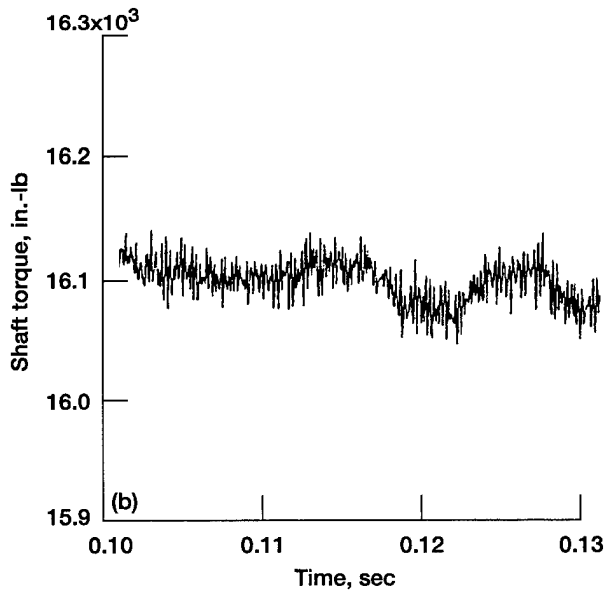
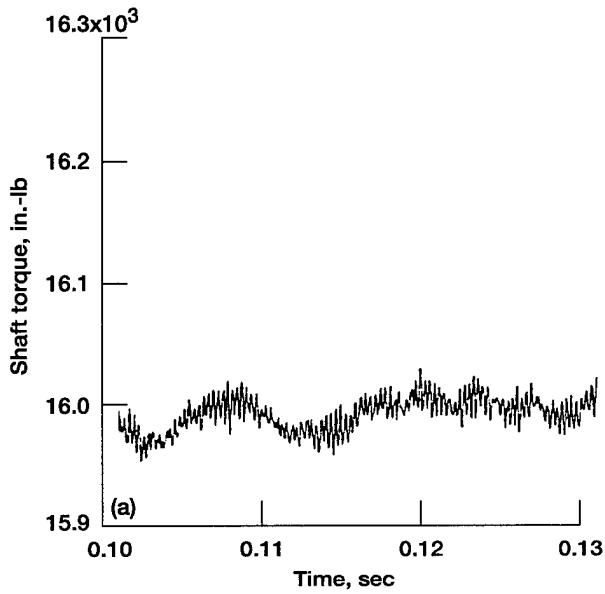


Fig. 10.—Shaft torques for 0° phasing of dual power paths showing baseline levels of torsional vibration. (a) Left compound shaft. (b) Right compound shaft.

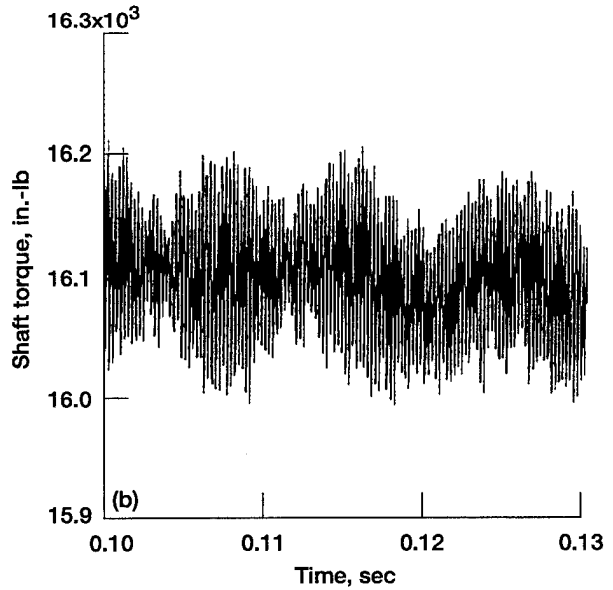
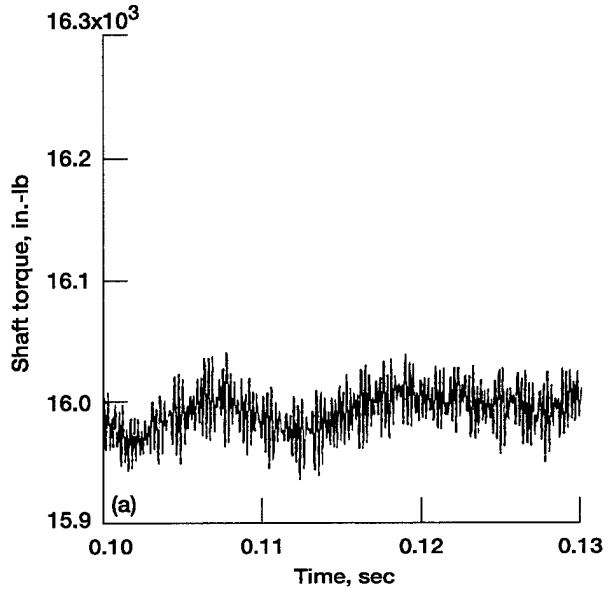


Fig. 11.—Shaft torques for 90° phasing of dual power paths showing large increase in torsional vibration of right power path. (a) Left compound shaft. (b) Right compound shaft.

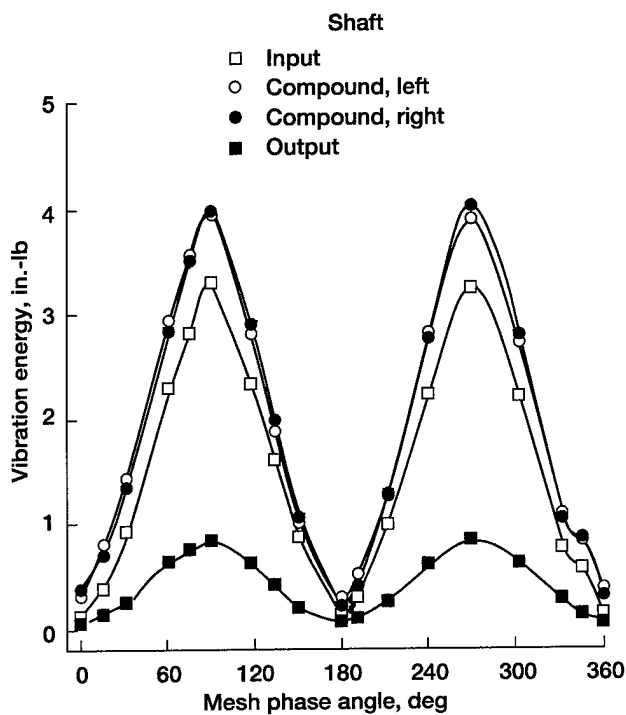


Fig. 12.—Energy of shaft lateral vibration as a function of mesh phase angle showing low vibration levels for 0° and 180° phase angles.

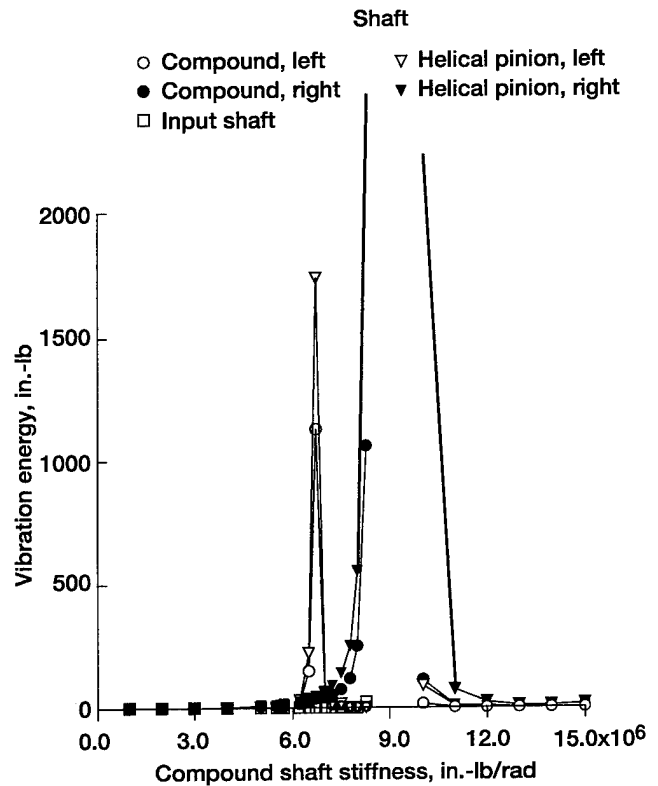


Fig. 14.—Energy of shaft torsional vibration as a function of compound shaft stiffness.

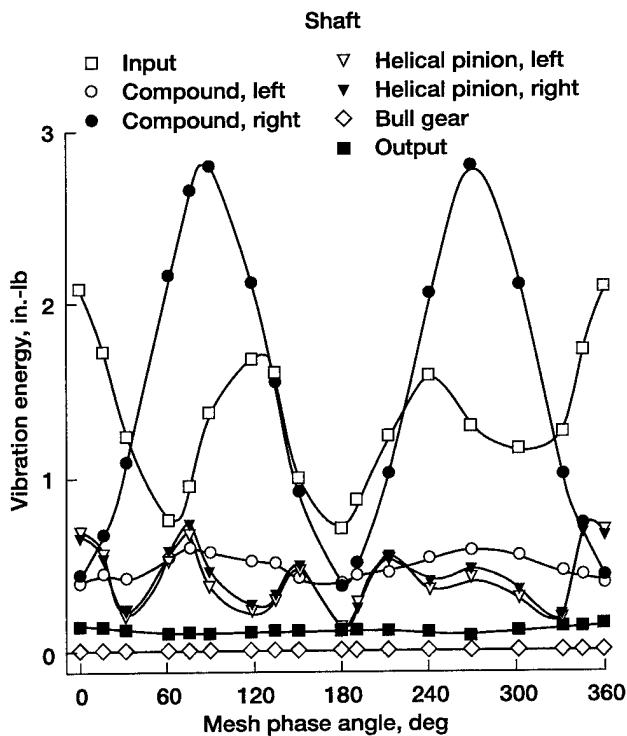


Fig. 13.—Energy of shaft torsional vibration as a function of mesh phase angle.

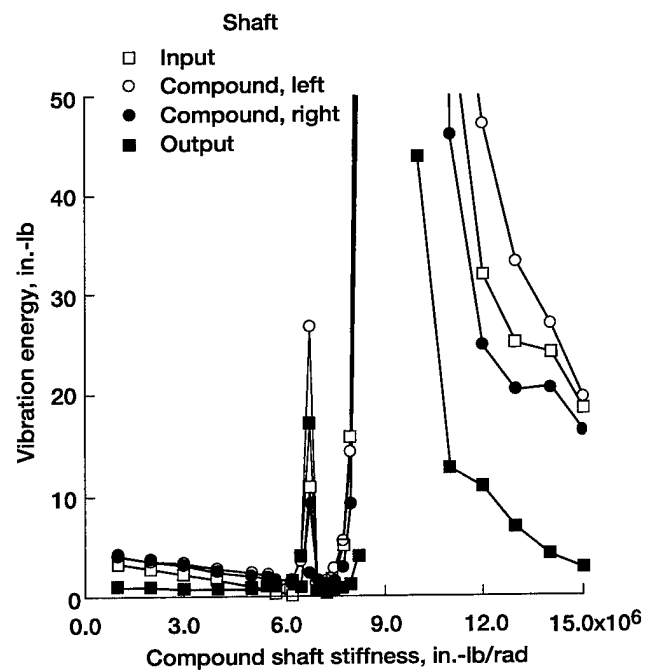


Fig. 15.—Energy of shaft lateral vibration as a function of compound shaft stiffness.

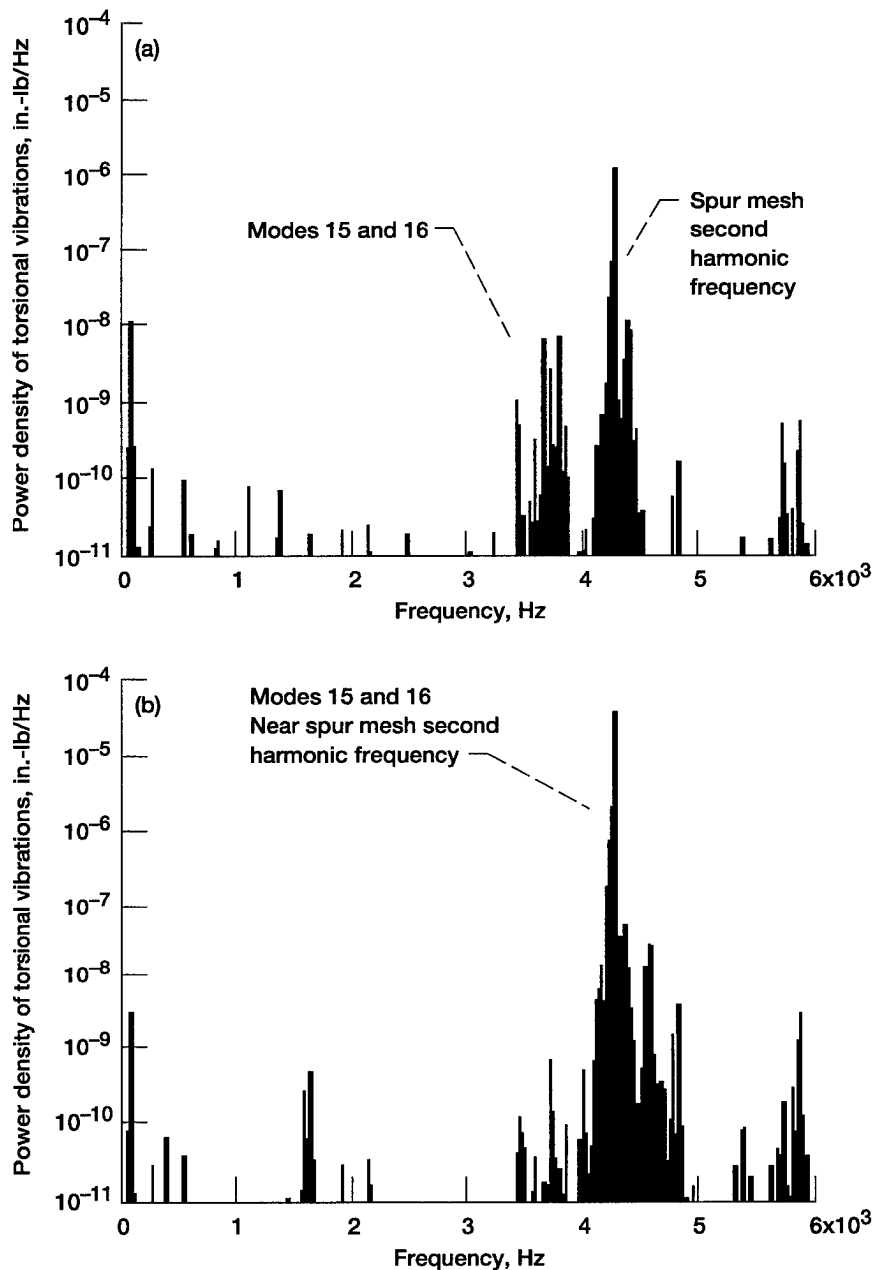


Fig. 16.—Spectrum of power density of shaft torsional vibration energy for right compound shaft at two stiffnesses. (a) Compound shaft stiffness = 3.0×10^6 in.-lb/rad. (b) Compound shaft stiffness = 7.8×10^6 in.-lb/rad.

The changes in the lateral vibration energy levels of four shafts are depicted in Fig. 15 as a function of the compound shaft stiffness. Note that although very strong torsional resonances were essentially limited to one of the two power paths, all four of the gearshafts had high lateral vibration levels when a resonance was excited. The power density frequency spectrum of the right compound shaft torsional vibration was calculated for the two values of shaft stiffnesses studied. These

two spectra are presented in Fig. 16. Note that at a shaft stiffness equal to 3.0×10^6 in.-lb/rad (Fig. 16(a)), the second harmonic of spur mesh frequency is strongly represented. There is also some energy at frequencies near the 15th and 16th natural frequencies even though they do not correspond to any mesh fundamental harmonic. This would indicate that the 15th and 16th modes are dominant ones for this system and that the second harmonic of mesh frequency is a strong excitation

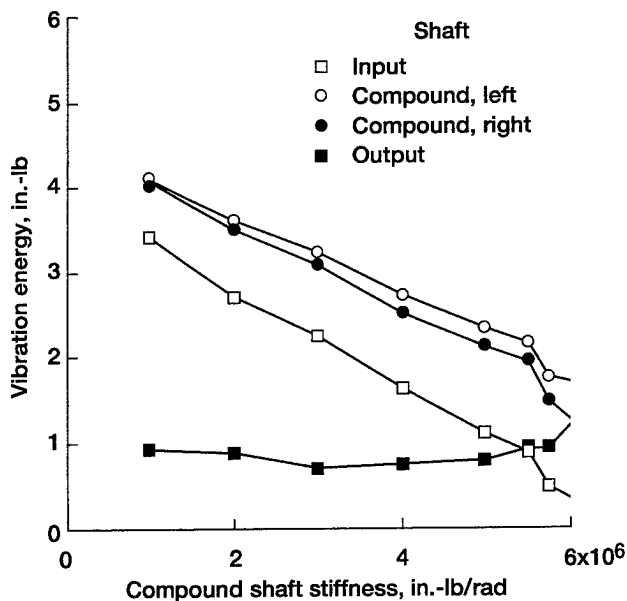


Fig. 17.—Energy of shaft lateral vibration as a function of compound shaft stiffness showing decreasing vibration with increasing stiffness over this range of values.

source. As the shaft stiffness is increased to 7.8×10^6 in.-lb/rad, the natural frequencies of the 15th and 16th modes fall very close to the second harmonic of the spur mesh fundamental and cause large torsional vibrations. The natural frequencies of these two dominant modes are significantly influenced by the stiffnesses of the compound shafts.

Referring again to Fig. 15, we note that, to achieve low levels of lateral vibration, the compound shaft stiffness should be selected such that the natural frequencies of the 15th and 16th modes are less than the frequency of the main excitation source (i.e., a shaft stiffness less than 6.0×10^6 in.-lb/rad). Making the 15th and 16th natural frequencies greater than the excitation source by selecting a very stiff compound shaft (i.e., near 15×10^6 in.-lb/rad) avoids the resonance condition but still results in relatively large vibration levels.

For the range of shaft stiffness from 1×10^6 to about 6×10^6 in.-lb/rad, the lateral vibration energy tends to decrease as the shaft stiffness is increased (Fig. 17). This contradicts Kish's experimental data⁸ for this gearbox, which showed that vibration of the gearbox tended to decrease as the shaft stiffness decreased. However, we must consider that the elastomeric device that produced the low shaft stiffness and low vibration in his experimental study also provided more damping than the all-steel device that produced high shaft stiffness and high vibration. In the analysis done here, damping was not considered; therefore, our results imply that in Kish's study⁸ the reduction in vibration level provided by the elastomeric device

was primarily a result of the increased damping and not the low torsional stiffness of the device.

Summary and Conclusions

A split path gearbox was studied by using an undamped, lumped spring and mass analytical model. Both frequency domain and time domain studies were done to determine the effects of three design variables (shaft angle, mesh phasing, and compound shaft stiffness) on the natural frequencies of vibration and vibration energy levels. For the time domain studies, the time-varying gear mesh properties were the source of vibration excitation. The equations of motion were derived by the Lagrangian method, and time domain studies were done using a fifth/sixth order Runge-Kutta method. The gearbox studied was the Advanced Rotorcraft Transmission Program split path test gearbox. The following observations and conclusions were drawn from the results of the dynamic analysis.

1. The mesh phasing strongly influenced the level of vibration energy. Mesh phasing at 0° and 180° produced low levels of lateral vibration, whereas mesh phasing at 90° and 270° produced relatively high vibration levels.
2. For the right compound shaft, both the lateral and torsional vibration levels varied as the mesh phasing varied; for the left compound shaft, the torsional vibration level remained relatively constant whereas the lateral vibration varied.
3. For the system studied here, the natural frequencies of two dominant modes of vibration were significantly influenced by the stiffness of the shafts that connect the spur gears to the helical pinions.
4. To achieve the lowest levels of vibration energy, the stiffnesses of the shafts connecting the spur gears to the helical pinions should be such that the natural frequencies of the dominant modes are less than the frequencies of the main excitation sources.
5. As the stiffnesses of the shafts connecting the spur gears to the helical pinions changed from about 1×10^6 to 6×10^6 in.-lb/rad, the vibration energy of lateral vibration decreased.
6. The reduction in vibration provided by the elastomeric device used by Kish was primarily due to increased damping, not the low stiffness of the device.
7. Most of the natural frequencies of vibration were not significantly influenced by varying the shaft angle.

Acknowledgements

The authors would like to thank J. Gene Kish and Charlie Isabelle of Sikorsky Aircraft for their interest and for their many discussions about helicopter drive systems and split path technology that contributed to this work.

References

1. White, G., "New Family of High-Ratio Reduction Gears with Multiple Drive Paths," Inst. Mech. Eng. (Lond.) Proc., Vol. 188, No. 23, 1974, pp. 281-288.
2. White, G., "Design of A 375 kW Helicopter Transmission with Split-Torque Epicyclic and Bevel Drive Stages," Inst. Mech. Eng. Proc., Part C, Mech. Eng. Sci., Vol. 197, Dec. 1983, pp. 213-224.
3. White, G., "Split-Torque Helicopter Transmission with Widely Separated Engines," Inst. Mech. Eng. Proc., Part G, J. Aero. Eng., Vol. 203, No. G1, 1989, pp. 53-65.
4. Hochmann, D., Houser, D.R., and Thomas, J., "Transmission Error and Load Distribution Analysis of Spur and Double Helical Gear Pairs Used in a Split Path Helicopter Transmission Design," Presented at AHS and Royal Aeronautical Society Technical Specialists' Meeting on Rotorcraft Acoustics/Fluid Dynamics, Philadelphia, Oct. 15-17, 1991.
5. Heath, G.F., and Bossler, R.B., "Advanced Rotorcraft Transmission (ART) Program—Final Report," NASA CR-191057, ARL-CR-4, 1993.
6. Krantz, T.L., "Dynamics of a Split Torque Helicopter Transmission, NASA TM-106410, ARL-TR-291, 1994.
7. Rashidi, M. and Krantz, T.L., "Dynamics of a Split Torque Helicopter Transmission," NASA TM-105681, AVSCOM TR-91-C-043, 1992.
8. Kish, J.G., "Sikorsky Aircraft Advanced Rotorcraft Transmission (ART) Program—Final Report," NASA CR-191079, ARL-CR-49, 1993.
9. Kahraman, A., "Dynamic Analysis of a Multi-mesh Helical Gear Train," Proceedings of the 1992 International Power Transmission and Gearing Conference, ASME DE, Vol. 43, Part 1, pp. 365-373.
10. Meirovitch, L., Elements of Vibration Analysis, McGraw-Hill, New York, 1975.
11. Cornell, R., "Compliance and Stress Sensitivity of Spur Gear Teeth," J. Mech. Des. Trans. ASME, Vol. 103, Apr. 1981, pp. 447-459.
12. IMSL User's Manual, Version 2.0, IMSL Inc., 1991.

REPORT DOCUMENTATION PAGE

Form Approved
OMB No. 0704-0188

Public reporting burden for this collection of information is estimated to average 1 hour per response, including the time for reviewing instructions, searching existing data sources, gathering and maintaining the data needed, and completing and reviewing the collection of information. Send comments regarding this burden estimate or any other aspect of this collection of information, including suggestions for reducing this burden, to Washington Headquarters Services, Directorate for Information Operations and Reports, 1215 Jefferson Davis Highway, Suite 1204, Arlington, VA 22202-4302, and to the Office of Management and Budget, Paperwork Reduction Project (0704-0188), Washington, DC 20503.

1. AGENCY USE ONLY (Leave blank)	2. REPORT DATE May 1995	3. REPORT TYPE AND DATES COVERED Technical Memorandum	
4. TITLE AND SUBTITLE Vibration Analysis of a Split Path Gearbox		5. FUNDING NUMBERS WU-505-62-36 1L162211A47A	
6. AUTHOR(S) Timothy L. Krantz and Majid Rashidi			
7. PERFORMING ORGANIZATION NAME(S) AND ADDRESS(ES) NASA Lewis Research Center Cleveland, Ohio 44135-3191 and Vehicle Propulsion Directorate U.S. Army Research Laboratory Cleveland, Ohio 44135-3191		8. PERFORMING ORGANIZATION REPORT NUMBER E-9498	
9. SPONSORING/MONITORING AGENCY NAME(S) AND ADDRESS(ES) National Aeronautics and Space Administration Washington, D.C. 20546-0001 and U.S. Army Research Laboratory Adelphi, Maryland 20783-1145		10. SPONSORING/MONITORING AGENCY REPORT NUMBER NASA TM-106875 ARL-TR-723 AIAA-95-3048	
11. SUPPLEMENTARY NOTES Prepared for the 31st Joint Propulsion Conference cosponsored by AIAA, SAE, and ASME, San Diego, California, July 10-12, 1995. Timothy L. Krantz, Vehicle Propulsion Directorate, U.S. Army Research Laboratory, NASA Lewis Research Center, and Majid Rashidi, Cleveland State University, Cleveland, Ohio 44115 (work funded under NASA Grant NAG3-1191). Responsible person, Timothy L. Krantz, organization code 2730, (216) 433-3580.			
12a. DISTRIBUTION/AVAILABILITY STATEMENT Unclassified - Unlimited Subject Category 37 This publication is available from the NASA Center for Aerospace Information, (301) 621-0390.		12b. DISTRIBUTION CODE	
13. ABSTRACT (Maximum 200 words) Split path gearboxes can be attractive alternatives to the common planetary designs for rotorcraft, but because they have seen little use, they are relatively high risk designs. To help reduce the risk of fielding a rotorcraft with a split path gearbox, the vibration and dynamic characteristics of such a gearbox were studied. A mathematical model was developed by using the Lagrangian method, and it was applied to study the effect of three design variables on the natural frequencies and vibration energy of the gearbox. The first design variable, shaft angle, had little influence on the natural frequencies. The second variable, mesh phasing, had a strong effect on the levels of vibration energy, with phase angles of 0° and 180° producing low vibration levels. The third design variable, the stiffness of the shafts connecting the spur gears to the helical pinions, strongly influenced the natural frequencies of some of the vibration modes, including two of the dominant modes. We found that, to achieve the lowest level of vibration energy, the natural frequencies of these two dominant modes should be less than those of the main excitation sources.			
14. SUBJECT TERMS Vibration; Dynamics; Gears; Bearings		15. NUMBER OF PAGES 17	
		16. PRICE CODE A03	
17. SECURITY CLASSIFICATION OF REPORT Unclassified	18. SECURITY CLASSIFICATION OF THIS PAGE Unclassified	19. SECURITY CLASSIFICATION OF ABSTRACT Unclassified	20. LIMITATION OF ABSTRACT

National Aeronautics and
Space Administration

Lewis Research Center
21000 Brookpark Rd.
Cleveland, OH 44135-3191

Official Business
Penalty for Private Use \$300

POSTMASTER: If Undeliverable — Do Not Return